Proceedings of the 9th World Congress on Mechanical, Chemical, and Material Engineering (MCM'23)
Brunel University, London, United Kingdom –August 06-08, 2023
Paper No. HTFF 218
DOI: 10.11159/htff23.218

Numerical Investigation of Heat Transfer and Fluid Flow Characteristics of Al_2O_3 Nanofluid In A Double Tube Heat Exchanger With Turbulator Insertion

Ebrahim Tavousi[1], Noel Perera[1], Dominic Flynn[2], Reaz Hasan[3]
[1]School of Engineering and the Built Environment, Faculty of Computing, Engineering and the Built Environment, Birmingham City University, Birmingham, B4 7XG, UK
Ebrahim.Tavousi@mail.bcu.ac.uk
[2]Vehicle Efficiency, Jaguar Land Rover, Gaydon, CV35 0BJ
[3]Department of Mechanical Engineering, Military Institute of Science and Technology, Dhaka, 1216, Bangladesh

Abstract **-** One of the primary objectives associated with the double tube heat exchanger is to enhance the heat transfer rate and improve the overall system performance. A promising approach to achieve these improvements involves combining turbulator insertion and nanofluid techniques. This study presents a numerical investigation that examines the impact of Al_2O_3-water nanofluid within the inner tube, along with turbulator insertion in the form of square-shaped ribs, on the heat transfer and fluid flow characteristics of the double tube heat exchanger. The findings indicate that an increase in the volume fraction of nanofluid leads to an enhanced heat transfer rate. Additionally, reducing the spacing between the turbulator ribs in the double tube heat exchanger results in an increase of up to 50% in the Nusselt number compared to a heat exchanger without turbulator insertion. The maximum performance evaluation criterion achieved in this study is 1.05.

Keywords**:** Double pipe heat exchanger, Heat transfer, Nanofluid, Nusselt number, Turbulator, Friction factor, Thermal efficiency

1. Introduction

A heat exchanger is a device used to transfer thermal energy between two or more fluids separated by solid material. One of the common heat exchangers is the double tube heat exchanger (DTHE). DTHEs are used to transfer heat between the cold and hot regions. These are used widely in industries and engineering applications such as refrigeration, air-conditioning, power plant, solar water heater, and the process industry [1-3]. One of the important challenges with heat exchangers is improving heat transfer capability [4-7].

Karimi [8] evaluated numerically the effect of twisted tape insertion and Al_2O_3-water nanofluid for the Reynolds number 250 to 2250 and 3000 to 9000 in a counter flow DTHE. The nanoparticle volume fractions were 1, 2, and 3%, and the cold nanofluid and superheat steam flowed in the inner and outer tubes, respectively. The results of the study demonstrated that the Nusselt number experienced a 22% increase as a result of twisted tape insertion alone and a 30% increase when a combination of twisted tape and nanofluid were employed, in comparison to the plain tube (without turbulator) and pure water conditions. Also, they concluded that using twisted tapes at high Reynolds numbers is more economical than low Reynolds numbers. Gnanavel [9] numerically studied the effect of heat transfer and fluid flow characteristics of spiral spring insertion and different nanofluids, including TiO_2, BeO, ZnO, and CuO, in a DTHE. In the conducted study, the Reynolds number range employed was from 1000 to 10000. The working fluids utilized were hot nanofluid and cold water, which were directed through the inner and outer tubes, respectively. The Nusselt number enhancements were obtained up to 117.39, 63.09, 56.63, and 47.62% for TiO_2, BeO, ZnO, and CuO, respectively. The maximum fiction factor increment was obtained for CuO with a value of 312%. The thermal performance factor decreased with the rise of the Reynolds number for all cases. Karuppasamy [10] investigated numerically the effect of cone shape insertion and Al_2O_3-water and CuO-water nanofluid on the performance of a DTHE. The volume fraction and range of Reynolds number were 1% and 2000 to 10000, respectively. The results showed that Al_2O_3-water gives a higher heat transfer rate than CuO-water, with the amount of 65% and 56%, respectively. The friction factor augmentation for Al_2O_3-water and CuO-water nanofluid were 50% and 47%.

In this study, the heat transfer characteristics and fluid flow behaviour of Al_2O_3-water nanofluid are investigated in a DTHE. Also, a turbulator insertion is implemented in the inner tube to investigate the effect of different distance of ribs on the performance of DTHE.

2. Governing equations

The governing equations of laminar flow in steady states for the single-phase model of nanofluid are continuity, momentum, and energy equations which define as follows [11].

For incompressible and steady flow, the continuity equation can be written as:

$$\frac{\partial u}{\partial x}+\frac{\partial v}{\partial y}+\frac{\partial w}{\partial z}=0 \tag{1}$$

The momentum equation for incompressible flow and constant viscosity, the equation can be written as:

$$\nabla.(\rho \boldsymbol{VV})=-\nabla P+\nabla.(\mu \nabla \boldsymbol{V}) \tag{2}$$

The conservation of energy for incompressible flow with constant thermal conductivity can be written as follow:

$$\nabla.(\rho \boldsymbol{V} C_p T)=\nabla.(k\nabla T) \tag{3}$$

Where ρ, k, and C_p represents density, thermal conductivity, and specific heat, respectively.

This study uses water-Al_2O_3 nanofluid as incompressible working fluid with constant physical characteristics. The physical properties of nanofluid are obtained based on nanoparticle volume fraction. The density and specific heat capacity [12-14], viscosity [15], and thermal conductivity of nanofluid [16] are calculated by the following equations [17]:

$$\rho_{nf}=(1-\varphi)\rho_b+\varphi\rho_p \tag{4}$$

$$(C_p)_{nf}=(1-\varphi)(C_p)_b+\varphi(C_p)_p \tag{5}$$

$$\mu=\frac{\mu_{nf}}{\mu_b}=123\varphi^2+7.3\varphi+1 \tag{6}$$

$$\frac{k_{nf}}{k_b}=4.97\varphi^2+2.72\varphi+1 \tag{7}$$

Where the subscripts of nf, b, and p refer to nanofluid, base fluid, and particles, respectively.

The local and average convection heat transfer coefficient in an internal flow with a radius of R_{in} can be obtained from the following equations [18].

$$h_{nf}=\frac{-k_{nf}\frac{\partial T}{\partial r}|_{r=R_{in}}}{T_{wall}-T_{b,nf}} \tag{8}$$

$$\overline{h_{nf}}=\frac{1}{L}\int_0^L h_{nf}.dx_{|r=R_{in}} \tag{9}$$

Where the subscript of b refers to bulk or mean quantity, and L is the tube length.

The local and average Nusselt number of nanofluid can be calculated from the following equations [19].

$$Nu_{nf}=\frac{h_{nf}(2R_{in})}{k_{in}} \tag{10}$$

$$\overline{Nu_{nf}}=\frac{\overline{h_{nf}}(2R_{in})}{k_{in}} \tag{11}$$

The Nusselt number empirical correlation for inner and outer tube based on laminar flow is defined as the following [20]:

$$Nu=1.86\left(RePr\frac{d}{L}\right)^{0.33} \tag{12}$$

Where the *Re, Pr, d and L* are the Reynolds, Prandtl number, tube diameter and length of DTHE, respectively.

The pressure drop in a tube with the length of L can be calculated from the following equation [21].

$$\Delta P=\frac{fL\rho V^2}{2d_h} \tag{13}$$

Where the d_h is the hydraulic diameter of the duct cross-section.

The PEC (Performance Evaluation Criteria) of DTHE can be obtained from the following equation [22].

$$PEC = \frac{\left(\frac{Nu}{Nu_0}\right)}{\left(\frac{f}{f_0}\right)^{1/3}} \quad (14)$$

Where the subscribe 0 refers to base fluid without nanoparticles.

3. Numerical method

The finite volume method was used to discretize the continuity, momentum, and energy equations for laminar forced convection in simulations. A coupled approach was used for velocity-pressure coupling, and a second-order upwind scheme was implemented for solving momentum and energy equations. Constant thermophysical properties are used for the single-phase Al_2O_3 nanofluid model.

Fig. 1 shows the schematic of a counter flow DTHE with turbulator insertion inside the inner tube. In this case, the length, inner, and outer tube diameter of the DTHE are 1.8 m, 0.014 m, and 0.08 m, respectively. A rod with a diameter of 0.002 m and 0.1 m for the first rib distance from the inlet was used to investigate the heat transfer rate and performance of the DTHE. The width (w) and height (h) of ribs are kept constant at 0.002 m, but the distance between ribs varies with the values 10, 8, 6, 4, and 2 cm. The cold Al_2O_3 nanofluid flows in the inner tube with a temperature of 283 k and Reynolds numbers 400 to 2000. The pure water with a temperature of 353 k and Reynolds number 800 as hot fluid flows in the outer tube. The outer tube wall was set as an adiabatic condition. The Al_2O_3-water nanofluid volume fractions are φ = 0, 0.025, 0.05, 0.075, and 0.1. The inner and outer tubes are considered cold nanofluid and hot water with velocity inlet boundary conditions at the inlet and pressure outlet at the end of the tube, respectively. The thermophysical properties of the working fluid, nanoparticles, and the material of the inner tube are given in Table 1.

Table 1: Thermophysical properties of used materials in this research.

Thermophysical properties	Water [23]	Al_2O_3 [24]	Copper [25]
ρ (J/kg K)	997.1	3970	8978
C_p (kg/m^3)	4179	765	381
k (W/m K)	0.613	40	387.6
μ (N s/m^2)	0.000891	-	-

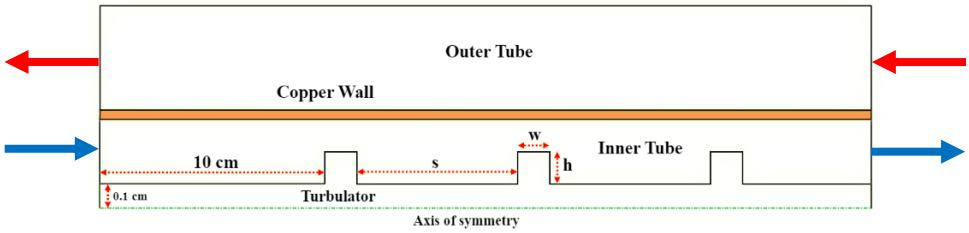

Figure 1 Schematic of the DTHE with turbulator insertion

4. Results and discussion

4.1. Grid independence and validation

In order to obtain a suitable number of meshes and mesh independence for simulations, the effect of meshes numbers on the heat transfer and hydrodynamic parameters was considered. The outlet temperature, average velocity, and pressure of the outlet for both the inner tube and outer tube were investigated for four different mesh densities (60k, 70k, 86k, and 158k). The results showed that the maximum change in temperature, velocity, and pressure values for other mesh densities compared to 60k number of cells is under 1%. Hence, the 60k number of cells was selected for all simulations to save time and cost.

The first validation was performed for the current study with an empirical correlation, which Seider and Tate [20] have proposed for the laminar flow and pure water (eq. 12). The results of the average Nusselt number in a counter flow configuration obtained from the equation eq. 12 were compared to the simulation results with Reynolds 400, 800, 1200, 1600, and 2000 for the inner side and constant Reynolds number 800 for the outer tube, with a constant 280 K and 350 K

inlet temperatures. In this case, the length, inner, and outer tube diameter of the DTHE are 1.8 m, 0.014 m, and 0.08 m, respectively.

Table. 2 shows the results for the first validation with the empirical results from Seider and Tate eq. 12 [20]. The deviation of results between the current study against empirical correlation was under 6%.

Table 2: Numerical vs empirical correlation results for Nusselt number in counter flow and different Reynolds number

Re	Nu (Numerical)	Nu (Experimental)	Error %
400	5.30	5.01	5.64
800	6.26	6.17	1.58
1200	7.06	7.05	0.16
1600	7.75	7.75	0.05
2000	8.36	8.34	0.22

For the second validation, the results of nanofluid simulations were compared to Bahmani, M.H. published work [26]. The average Nusselt number in a counter flow configuration for Reynolds numbers 100, 200, 500, 100, and 1500 for the inner tube with a constant Reynolds number 500 for the outer tube and with a constant 283 K and 353 K inlet temperatures were compared to the current simulations. In this case, the length, inner, and outer tube diameter of the DTHE are 2 m, 0.026 m, and 0.05 m, respectively.

Fig. 2 shows the results for the second validation with Bahmani, M.H. published work [26]. The deviation of results between the current study against Bahmani, M.H. was under 12%.

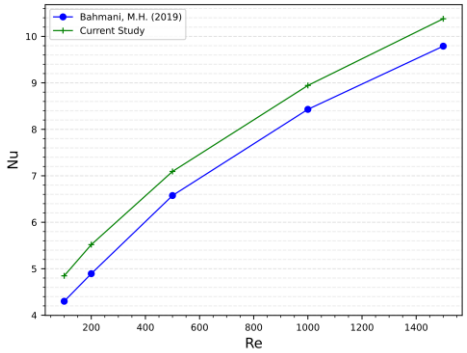

Figure 2 validation of present study with numerical results of Bahmani, M.H. *[26]* for counter flow

The successful validation of the simulation results using both experimental and numerical methods ensure the reliability and accuracy of the simulations for other cases.

4.2. Effect of turbulator insertion and nanoparticle volume fraction on DTHE

Fig. 3 shows the results of the average Nusselt number against the Reynolds number for different nanoparticle volume fractions. It is observed that the average Nusselt number increases with an increase in the nanoparticles volume fractions and Reynolds number. Furthermore, it is evident that the inclusion of turbulators in the inner tube leads to an increase in the Nusselt number. This augmentation can be attributed to the enhanced thermophysical properties of the nanofluid, as well as the generation of secondary flow and mixing flow resulting from the presence of the turbulators.

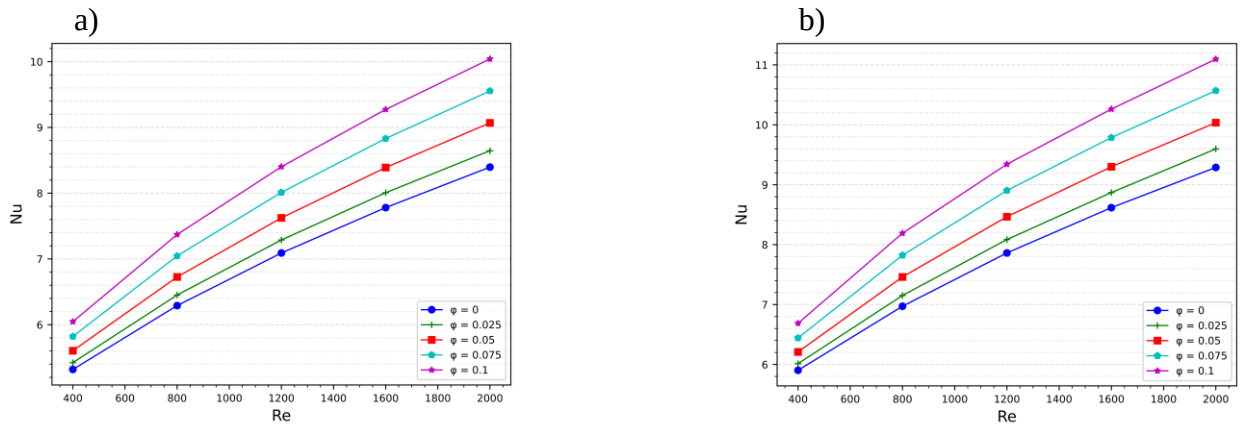

Figure 3 Nusselt number against Reynolds number for a) no turbulator insertion b) s=10 cm

Fig. 4 illustrates the effect of various nanoparticle volume fractions and Reynolds number for the pressure drop of the inlet and outlet of the inner tube. It can be concluded that increasing nanoparticle volume fraction and Reynolds number increases pressure drop. Also, by adding turbulator insertion, the pressure drop increase along the inner tube. The increase in the pressure drop is due to the higher surface area of ribs and reverse flow that creates the dissipation of dynamic pressure in the fluid. The increase of nanofluid viscosity due to adding nanoparticles in the base fluid is another reason for the increase in the pressure drop.

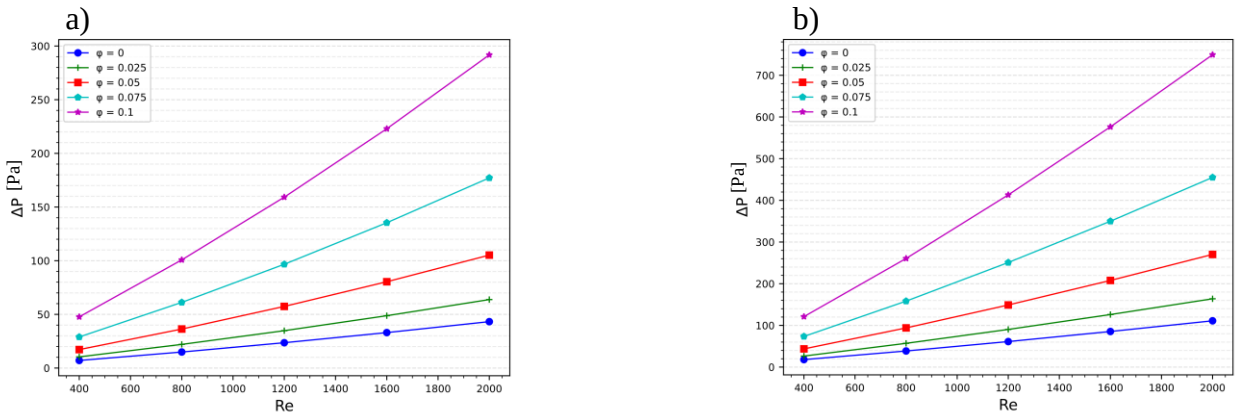

Figure 4 Pressure drop against Reynolds number a) no turbulator insertion b) s=10 cm

Fig. 5 represents the average Nusselt number against different distances between the ribs for different Reynolds numbers and Reynolds numbers. The results show that decreasing the distance between ribs increases the Nusselt number. There is a significant enhancement between s=2 cm and s=4,6,8,10 cm, which shows the effective distance between ribs due to the flow separation. Additionally, decreasing the distance between the ribs increases the number of ribs, which leads to an increase in the mixing of flow and subsequently an increase in the Nusselt number.

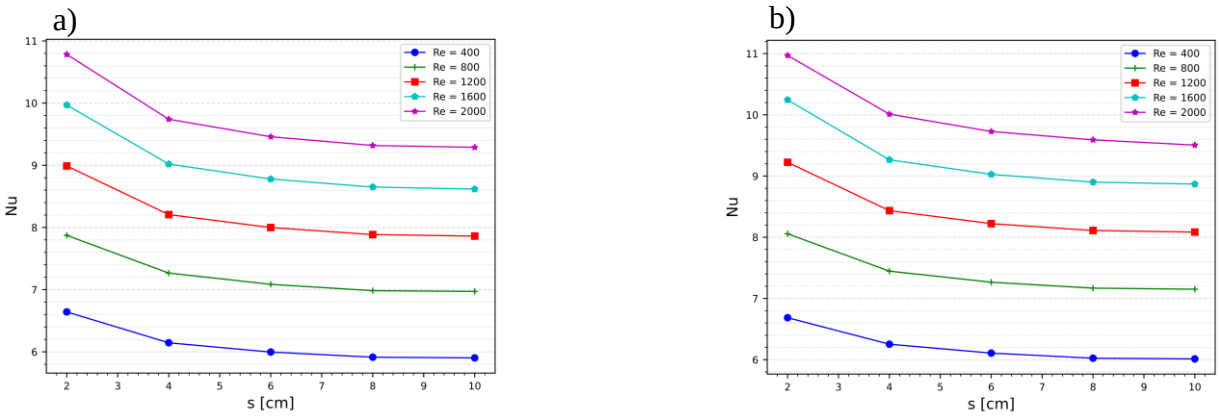

Figure 5 Nusselt number against different distances between the ribs a) φ=0 b) φ=0.025

Fig. 6 shows the PEC of DTHE against the Reynolds number for varying nanoparticle volume fractions and different distances between the ribs. The findings reveal an increase in the nanoparticle volume fraction and the distance between the ribs leads to higher values of the PEC. Reducing the distances between the ribs and increasing their quantity has a more significant impact on the friction factor increment than the observed rise in the Nusselt number.

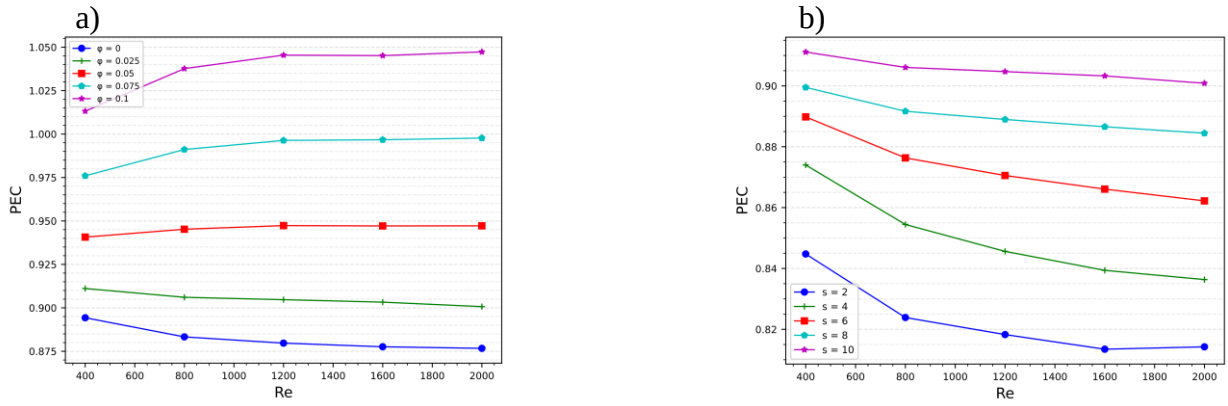

Figure 6 PEC against Reynolds number a) s=10 cm b) φ=0.025

Fig. 7 shows the colour plots of static pressure, velocity magnitude, static temperature, and streamline of the inner and outer tubes in the DTHE. The Reynolds number, nanofluid volume fraction, and distance between ribs are 800, 0.1, and s=2 cm, respectively. The velocity magnitude and streamline graph indicate how ribs make obstacles and deviate in the flow. These effects induce turbulence and secondary flow that reduce the thermal boundary layer and increase the heat transfer rate in the DTHE.

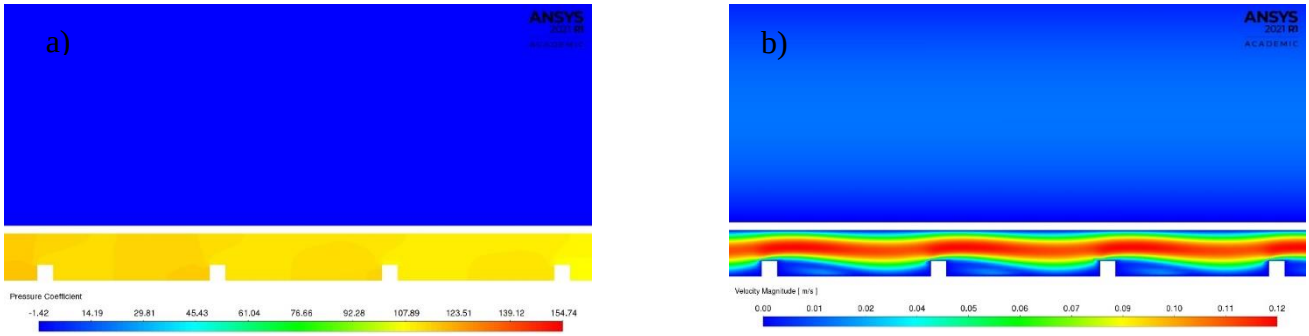

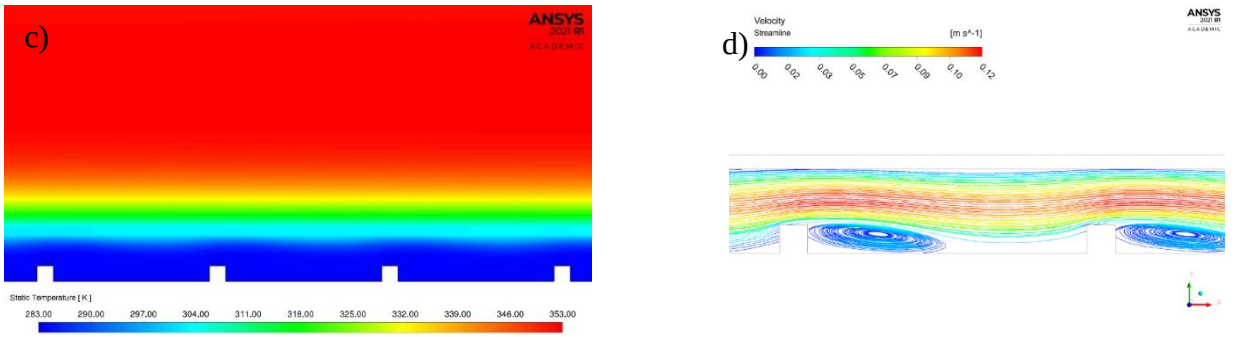

Figure 7 colour plots of a) static pressure b) velocity c) static temperature d) streamline for Re=800, φ=0.1, and s=2 cm

Fig. 8 represents the maximum enhancement of the average Nusselt number and friction factor for the combination of nanofluid and the distance between the ribs of the turbulator insertion compared to the pure water. The maximum average Nusselt number enhancement and friction factor increment occur in the s=2 cm, 0.1 nanoparticle volume fraction, and highest Reynolds number with values of about 50% and 300%, respectively. This can be attributed to the presence of a larger number of ribs, which promote higher levels of turbulence and mixing in the flow, as well as the increased viscosity of the nanofluid.

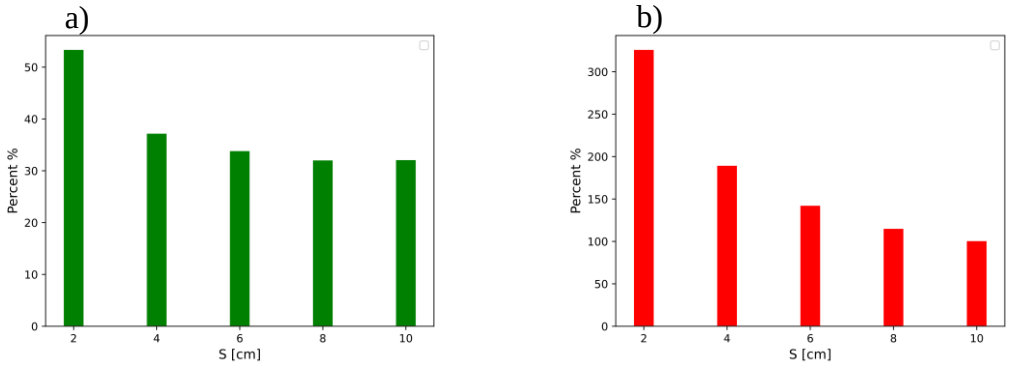

Figure 8 Maximum a) Nusselt number enhancement b) friction factor increment

5. Conclusion

The important results of the study can be summarized as follows:

- The Nusselt number, and pressure drop increased proportionally to an increase in the volume fraction and Reynolds number.
- With the turbulator insertion, the Nusselt number and pressure drop increased with a decrease in the distance between ribs.
- The highest PEC achieved for the combination of turbulator insertion and nanofluid was 1.05 at s=10 cm.
- The highest average Nusselt number enhancement of 53.43% was observed in the combination of turbulator insertion and nanofluid.

Acknowledgements

The authors declare that they have no known competing financial interests or personal relationships that could have appeared to influence the work reported in this paper.

References

[1] H. Mohammed, H. A. Hasan, and M. Wahid, "Heat transfer enhancement of nanofluids in a double pipe heat exchanger with louvered strip inserts," *International Communications in Heat and Mass Transfer*, vol. 40, pp. 36-46, 2013.

[2] S. Kakac, H. Liu, and A. Pramuanjaroenkij, *Heat exchangers: selection, rating, and thermal design*. CRC press, 2002.

[3] R. K. Shah and D. P. Sekulic, *Fundamentals of heat exchanger design*. John Wiley & Sons, 2003.
[4] S. Liu and M. Sakr, "A comprehensive review on passive heat transfer enhancements in pipe exchangers," *Renewable and sustainable energy reviews,* vol. 19, pp. 64-81, 2013.
[5] W. M. Rohsenow, J. P. Hartnett, and Y. I. Cho, *Handbook of heat transfer*. McGraw-Hill New York, 1998.
[6] F. Lalegani, M. R. Saffarian, A. Moradi, and E. Tavousi, "Effects of different roughness elements on friction and pressure drop of laminar flow in microchannels," *International Journal of Numerical Methods for Heat & Fluid Flow,* vol. 28, no. 7, pp. 1664-1683, 2018.
[7] E. Tavousi, N. Perera, D. Flynn, and R. Hasan, "Heat transfer and fluid flow characteristics of the passive method in double tube heat exchangers: a critical review," *International Journal of Thermofluids*, p. 100282, 2023.
[8] A. Karimi, A. A. Al-Rashed, M. Afrand, O. Mahian, S. Wongwises, and A. Shahsavar, "The effects of tape insert material on the flow and heat transfer in a nanofluid-based double tube heat exchanger: two-phase mixture model," *International Journal of Mechanical Sciences,* vol. 156, pp. 397-409, 2019.
[9] C. Gnanavel, R. Saravanan, and M. Chandrasekaran, "Heat transfer augmentation by nano-fluids and Spiral Spring insert in Double Tube Heat Exchanger–A numerical exploration," *Materials Today: Proceedings,* vol. 21, pp. 857-861, 2020.
[10] M. Karuppasamy, R. Saravanan, M. Chandrasekaran, and V. Muthuraman, "Numerical exploration of heat transfer in a heat exchanger tube with cone shape inserts and Al2O3 and CuO nanofluids," *Materials Today: Proceedings,* vol. 21, pp. 940-947, 2020.
[11] M. Iwaniszyn *et al.*, "Entrance effects on forced convective heat transfer in laminar flow through short hexagonal channels: Experimental and CFD study," *Chemical Engineering Journal,* vol. 405, p. 126635, 2021.
[12] O. A. Akbari, D. Toghraie, A. Karimipour, A. Marzban, and G. R. Ahmadi, "The effect of velocity and dimension of solid nanoparticles on heat transfer in non-Newtonian nanofluid," *Physica E: Low-Dimensional Systems and Nanostructures,* vol. 86, pp. 68-75, 2017.
[13] A. Kamyar, R. Saidur, and M. Hasanuzzaman, "Application of computational fluid dynamics (CFD) for nanofluids," *International Journal of Heat and Mass Transfer,* vol. 55, no. 15-16, pp. 4104-4115, 2012.
[14] T. Bergman, "Effect of reduced specific heats of nanofluids on single phase, laminar internal forced convection," *International Journal of heat and mass Transfer,* vol. 52, no. 5-6, pp. 1240-1244, 2009.
[15] H. Alipour, A. Karimipour, M. R. Safaei, D. T. Semiromi, and O. A. Akbari, "Influence of T-semi attached rib on turbulent flow and heat transfer parameters of a silver-water nanofluid with different volume fractions in a three-dimensional trapezoidal microchannel," *Physica E: Low-Dimensional Systems and Nanostructures,* vol. 88, pp. 60-76, 2017.
[16] S. E. B. Maïga, C. T. Nguyen, N. Galanis, G. Roy, T. Maré, and M. Coqueux, "Heat transfer enhancement in turbulent tube flow using Al2O3 nanoparticle suspension," *International Journal of Numerical Methods for Heat & Fluid Flow,* 2006.
[17] B. C. Pak and Y. I. Cho, "Hydrodynamic and heat transfer study of dispersed fluids with submicron metallic oxide particles," *Experimental Heat Transfer an International Journal,* vol. 11, no. 2, pp. 151-170, 1998.
[18] J. Lin, Y. Hong, and J. Lu, "New method for the determination of convective heat transfer coefficient in fully-developed laminar pipe flow," *Acta Mechanica Sinica,* vol. 38, no. 1, pp. 1-10, 2022.
[19] H. E. Ahmed, M. Ahmed, I. M. Seder, and B. Salman, "Experimental investigation for sequential triangular double-layered microchannel heat sink with nanofluids," *International Communications in Heat and Mass Transfer,* vol. 77, pp. 104-115, 2016.
[20] E. N. Sieder and G. E. Tate, "Heat transfer and pressure drop of liquids in tubes," *Industrial & Engineering Chemistry,* vol. 28, no. 12, pp. 1429-1435, 1936.
[21] F. M. White, *Fluid mechanics*. Tata McGraw-Hill Education, 1979.

[22] M. Noorbakhsh, S. S. M. Ajarostaghi, M. Zaboli, and B. Kiani, "Thermal analysis of nanofluids flow in a double pipe heat exchanger with twisted tapes insert in both sides," *Journal of Thermal Analysis and Calorimetry*, vol. 147, no. 5, pp. 3965-3976, 2022.

[23] O. A. Akbari, D. Toghraie, and A. Karimipour, "Impact of ribs on flow parameters and laminar heat transfer of water–aluminum oxide nanofluid with different nanoparticle volume fractions in a three-dimensional rectangular microchannel," *Advances in Mechanical Engineering*, vol. 7, no. 11, p. 1687814015618155, 2015.

[24] O. A. Akbari *et al.*, "Investigation of rib's height effect on heat transfer and flow parameters of laminar water–Al2O3 nanofluid in a rib-microchannel," *Applied Mathematics and Computation*, vol. 290, pp. 135-153, 2016.

[25] L.-L. Tian, X. Liu, S. Chen, and Z.-G. Shen, "Effect of fin material on PCM melting in a rectangular enclosure," *Applied Thermal Engineering*, vol. 167, p. 114764, 2020.

[26] M. H. Bahmani, O. A. Akbari, M. Zarringhalam, G. A. S. Shabani, and M. Goodarzi, "Forced convection in a double tube heat exchanger using nanofluids with constant and variable thermophysical properties," *International Journal of Numerical Methods for Heat & Fluid Flow*, 2019.